

# Azo Anion Radical Complex of Rhodium as a Molecular Memory Switching Device: Isolation, Characterization, and Evaluation of Current–Voltage Characteristics

Nanda D. Paul,<sup>†</sup> Utpal Rana,<sup>‡</sup> Sreetosh Goswami,<sup>§</sup> Tapan K. Mondal,<sup>||</sup> and Sreebrata Goswami<sup>\*,†</sup>

<sup>†</sup>Department of Inorganic Chemistry, Indian Association for the Cultivation of Science, Jadavpur, Kolkata 700 032, India

<sup>‡</sup>Polymer Science Unit, Indian Association for the Cultivation of Science, Jadavpur, Kolkata 700 032, India

<sup>§</sup>Department of Electrical Engineering, Bengal Engineering and Science University, Howrah 711 103, India

<sup>||</sup>Department of Chemistry, Jadavpur University, Jadavpur, Kolkata 700 032, India

## Supporting Information

**ABSTRACT:** Two rare examples of azo anion diradical complexes of Rh(III) are reported. These complexes showed excellent memory switching properties with a large ON/OFF ratio and are suitable for RAM/ROM applications. Their electronic structures have been elucidated using a host of physical methods, including X-ray crystallography, variable-temperature magnetic susceptibility measurement, cyclic voltammetry, electron paramagnetic resonance spectroscopy, and density functional theory. The results indicate a predominant triplet state description of the systems with two ferromagnetically coupled radicals.

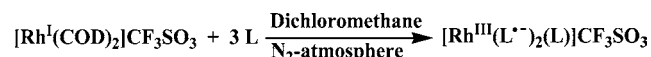
During recent years, the invention of thin-film devices with memristive properties<sup>1</sup> has led to a revolutionary turn in the research area of electrical switching technology.<sup>2</sup> This is because such a technology may enable functional scaling of logic and memory circuits well beyond the limits of complementary metal–oxide–semiconductors and have the potential to simulate biological and neuromorphical processes as well.<sup>1a,2,3</sup> Herein we disclose the first-ever example of a metal-stabilized organic radical system that exhibits memristive properties.

Because of their diverse chemical and physical properties, organic radicals are at the focus of contemporary research.<sup>4</sup> They are highly reactive, and their isolation in the crystalline state has always been a challenge. In this respect, a strategy of using transition-metal ions with multivalent possibilities<sup>4a–c,5</sup> as a carrier of radical ligands has been successfully used. Consequently, a large variety of transition-metal-stabilized radical complexes have been synthesized. However, in most cases the radical character of the coordinated ligand is obscured through the coupling of the radical spin with unpaired electrons on the metal or on another radical ligand.<sup>6</sup> Thus, stable, uncoupled radical complexes are rare in the literature.

During our recent works on non-redox-innocent aromatic azo ligands, we have developed a synthetic protocol<sup>6a–c,7</sup> for the synthesis of metal-stabilized azo anion radical complexes using low-valent transition-metal precursors. Accordingly, the diradical complexes  $[\text{Rh}^{\text{III}}(\text{L}^{\bullet-})_2(\text{L})]\text{CF}_3\text{SO}_3$  (**[1]** $\text{CF}_3\text{SO}_3$ ; R = H (**1a**), Cl (**1b**), where R is a substituent on the pendant

phenyl ring of the ligand L) were synthesized in excellent yields (>90%) from the reaction of the substitutionally labile, electron-rich precursor  $[\text{Rh}^{\text{I}}(\text{COD})_2]\text{CF}_3\text{SO}_3$  with 2-(aryloxy)pyridine [L; R = H, L<sup>a</sup> = 2-(phenylazo)pyridine; R = Cl, L<sup>b</sup> = 2-(4-chlorophenylazo)pyridine] in a dry nitrogen atmosphere (Scheme 1).

## Scheme 1. Synthetic Reaction



Microanalytical positive-ion electrospray ionization mass spectra of the two compounds convincingly support their formulation [see the Supporting Information (SI)]. The X-ray structure of the representative complex **[1b]** $\text{CF}_3\text{SO}_3$  was solved, and the molecular view is displayed in Figure 1 (for

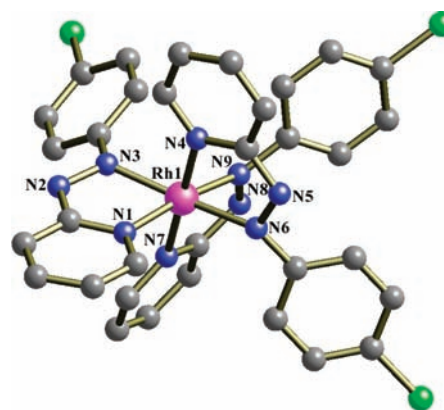


**Figure 1.** Molecular view of the complex **[1b]** $\text{CF}_3\text{SO}_3$ . H atoms and  $\text{CF}_3\text{SO}_3$  have been omitted for clarity. Selected bond lengths (Å): Rh1–N1, 2.015(2); Rh1–N3, 2.034(2); Rh1–N4, 2.037(2); Rh1–N6, 2.061(2); Rh1–N7, 2.015(2); Rh1–N9, 2.072(2); N2–N3, 1.341(3); N5–N6, 1.277(3); N8–N9, 1.332(3).

the ORTEP, see Figure S2 in the SI). The structural analysis revealed that the complex **[1b]** $\text{CF}_3\text{SO}_3$  is hexacoordinate, with

Received: December 31, 2011

Published: March 30, 2012

the central metal ion residing in a distorted octahedral environment. The most notable part of the structure is the unusual elongation of the N–N (azo) bonds in two of the three coordinated ligands; the three N–N bond lengths ( $d_{\text{N-N}}$ ) are 1.341(3), 1.332(3), and 1.277(3) Å (Table S3 in the SI). Notably, the N–N distance is an excellent indicator of the charge of an azo function. From the  $d_{\text{N-N}}$  of ca. 1.24 Å for free ligands,<sup>8</sup> coordination by back-donating metals may shift this value to ca. 1.25–1.30 Å. Real one-electron-reduced (i.e., anion radical) ligands have  $d_{\text{N-N}} \approx 1.35$  Å, while the two-electron-reduced hydrazido(2-) ligands have single bonds with  $d_{\text{N-N}} > 1.40$  Å. The observation of the two elongated azo chromophores clearly is in accordance with the anion radical form of the two coordinated ligands and, by implication, the trivalent state for the metal in  $[\text{Rh}^{\text{III}}(\text{L}^{\bullet-})_2(\text{L})]\text{CF}_3\text{SO}_3$ .

The magnetic properties of the complexes were probed by variable-temperature magnetic moment measurements (Figure 2a). At 300 K, the value of  $\mu_{\text{eff}}$  ( $2.42 \mu_{\text{B}}$ ) is close to that

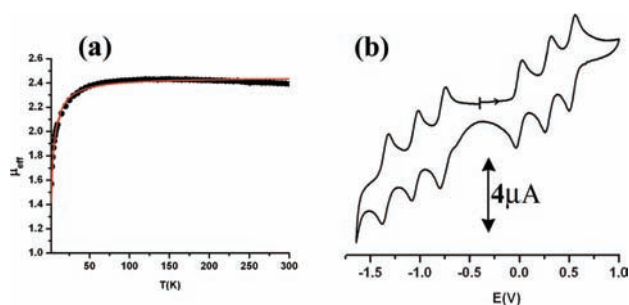


**Figure 2.** (a) Plot of  $\mu_{\text{eff}}$  (black ● for experimental data, red line for theoretical value) vs  $T$  for  $[\mathbf{1b}]\text{CF}_3\text{SO}_3$ . (b) Cyclic voltammogram of  $[\mathbf{1a/b}]\text{CF}_3\text{SO}_3$  in  $\text{CH}_2\text{Cl}_2/0.1 \text{ M Bu}_4\text{NClO}_4$  with a Pt working electrode and a saturated Ag/AgCl reference electrode.

calculated for two uncoupled  $S = 1/2$  spins with  $g = 2.0$ .<sup>9</sup> The effective magnetic moment for  $[\mathbf{1b}]\text{CF}_3\text{SO}_3$  increases very slightly with decreasing temperature and reaches a maximum value of  $2.44 \mu_{\text{B}}$  near 100 K, revealing the presence of a weak ferromagnetic interaction between the two radical magnetic centers. At much lower temperatures (<50 K), the magnetic moment decreases rapidly because of the intermolecular antiferromagnetic interaction. Theoretical modeling of the experimental data using the Bleaney–Bowers equation<sup>9</sup> with the isotropic exchange Hamiltonian ( $\hat{H} = -J\hat{S}_1\cdot\hat{S}_2$ ) for the two interacting  $S = 1/2$  centers yielded  $J = 2.15 \text{ cm}^{-1}$  ( $J$  is the exchange constant between the two radical ligands) and  $\theta = -5.0 \text{ K}$  ( $\theta$  is the intermolecular exchange coupling constant) (see the SI). The triplet spin state was further characterized by electron paramagnetic resonance (EPR) spectroscopy in a dichloromethane/toluene glass at 77 K (Figure S3). The EPR spectra of  $[\mathbf{1a/b}]\text{CF}_3\text{SO}_3$  show a broad, nearly isotropic signal with an additional weak spin-forbidden  $\Delta m_s = \pm 2$  transition at half field.<sup>10</sup> In variable-temperature measurements, the intensity of the spectrum increased as the temperature was lowered to 77 K. This overall increase in intensity and especially the increase in the low-field transition is consistent with the ferromagnetically coupled diradical nature of  $[\mathbf{1a/b}]\text{CF}_3\text{SO}_3$ .<sup>10c,d</sup>

Cyclic voltammetry of the complexes  $[\mathbf{1a/b}]\text{CF}_3\text{SO}_3$  in  $\text{CH}_2\text{Cl}_2$  exhibited six reversible one-electron redox responses (three oxidation and three reduction) in the potential range 1.0 to  $-1.5 \text{ V}$  (Figure 2b and Table S2). The first two anodic responses are due to the oxidation of the two coordinated

radicals, and the third wave is attributed to the oxidation of Rh(III) to Rh(IV); the corresponding cathodic responses are ascribed to the stepwise reductions of the three coordinated ligands.<sup>7</sup> The uncoordinated free azo ligand, under identical experimental conditions, showed two cathodic responses near  $-1.06$  and  $-1.86 \text{ V}$  (Table S2 and Figure S4). These are due<sup>6a-d,7</sup> to its stepwise reduction to the azo anion radical and dianionic hydrazido forms, respectively.

To elucidate further the electronic structure of the complexes, broken-symmetry (BS) hybrid density functional theory (DFT) calculations were conducted on  $[\mathbf{1b}]\text{CF}_3\text{SO}_3$  at the B3LYP level.<sup>11</sup> The calculated bond characteristics for the triplet ground state (Table S3) are in reasonable agreement with the experimental values. The singlet state was found to reside much higher in energy ( $12.87 \text{ kcal mol}^{-1}$ ) relative to the triplet state. In  $[\mathbf{1b}]\text{CF}_3\text{SO}_3$ , two ligand radicals were observed in the spin density maps, which featured typical patterns for azo anion radicals,<sup>6a</sup> indicating that two ligands carry one unpaired electron each, leaving the third one in the unreduced neutral form (Figure 3). The LUMOs are also localized on the ligands

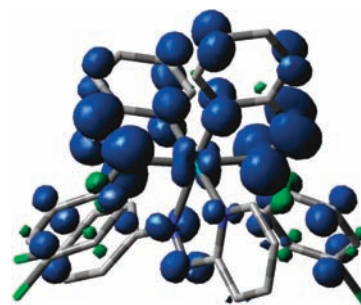


**Figure 3.** Spin density plot for  $[\mathbf{1b}]\text{CF}_3\text{SO}_3$  in the native  $S = 1$  state ( $S^2 = 2.0222$ ; spin populations: Rh, 0.0600; L, 0.1580;  $\text{L}^{\bullet-}$ , 0.8036;  $\text{L}^-$ , 0.9784).

(Tables S5 and S6 and Figures S7 and S8). These results are in line with the structural features of the complexes (Table S3) and confirm the direct participation of the ligands in the redox processes, as stressed by the electrochemical measurements. The spin density map for the theoretical model of the native  $[\mathbf{1b}]\text{CF}_3\text{SO}_3$  is shown in Figure 3. The calculated structural parameters (Table S3), the composition of the molecular orbitals (Tables S5 and S6 and Figures S7 and S8), and the spin density plots of the redox partners  $[\mathbf{1b}]^{2+}$ ,  $[\mathbf{1b}]^{3+}$ ,  $[\mathbf{1b}]^{4+}$ ,  $[\mathbf{1b}]$ ,  $[\mathbf{1b}]^-$ , and  $[\mathbf{1b}]^{2-}$  (Figures S9–S12) are consistent with ligand-based redox processes, with the exception that the third oxidation process occurs at the metal center [Rh(III)  $\rightarrow$  Rh(IV)]. Furthermore, the EPR spectra of the above electrogenerated complexes also support these descriptions. A detailed analysis of the spectroelectrochemical studies will be published separately in a future publication.

Thus, the complexes  $[\mathbf{1}]\text{CF}_3\text{SO}_3$  with multiple reversible electron transfer processes were anticipated to be suitable candidates for possible application as a molecular memory device.<sup>12</sup> Accordingly, a device was prepared as shown in Figure 4a and tested for the above possible application. It consisted of chloroform solution spin-coated  $[\mathbf{1b}]\text{CF}_3\text{SO}_3$  film (100 nm) sandwiched between two gold electrodes (see the Experimental Section in the SI). The selection of two identical electrodes allowed us a clear demonstration of whether or not the origin of the memory effect comes from an intrinsic property of the

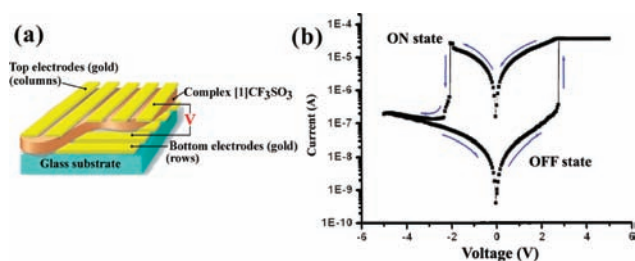


**Figure 4.** (a) Cross-sectional view of the device layout for the memory device. (b) Current–voltage ( $I$ – $V$ ) characteristics of the Au/[**1b**]CF<sub>3</sub>SO<sub>3</sub>/Au molecular device (semilogarithmic scale).

diradical complex [**1b**]CF<sub>3</sub>SO<sub>3</sub>.<sup>12a</sup> The thicknesses of the top and bottom electrodes were 90 and 85 nm, respectively.

The current–voltage ( $I$ – $V$ ) characteristics of the device (Figure 4b) were recorded in the range  $V = +5$  to  $-5$  V at a scan rate of 10 mV/s using a potential sweep in the positive to negative direction with a bias being applied on a film of thickness 100 nm (Figure S6). In the voltage sweep from 0 to  $+5$  V, an abrupt increase in current was observed at a switching threshold voltage of 2.75 V, indicating the device transition from a low-conductivity (OFF) state to a high-conductivity (ON) state (“writing” process), and this state was retained until a negative bias threshold voltage of  $-2.05$  V was applied, at which there was an abrupt decrease in current indicating the device transition from the ON state to the OFF state (“erasing” process). The erased state (OFF) could be rewritten (ON) by applying the switching threshold voltage. It is indeed interesting to note that the distinct bielectrical states in the voltage range  $-2.05$  to  $+2.75$  V allow any voltage in this range to read as an OFF or ON signal depending upon the history of the voltage sweep, which actually qualifies the device to be used as nonvolatile memory device.

For comparison, the  $I$ – $V$  characteristics of the free azo ligand (**L<sup>b</sup>**) (Figure S5) do not show any switching in the voltage range  $V = +5$  to  $-5$  V. It may be concluded that the switching phenomenon reported herein is a molecular property of the diradical complex. The mechanism of the switching process remains unresolved as yet. However, it may be proposed that the switching-ON process is due to the shifting of electrode Fermi levels with the applied potential and their alignment with the donor and acceptor orbitals of the materials,<sup>12b,13</sup> resulting in a high-conducting state. In this state (ON), the device behaves as an ohmic material during the voltage sweep from  $+2.75$  V to  $-2.05$  V, at which (i.e.,  $-2.05$  V) the material switches to the low-conducting (OFF) state.

The device can be used as random-access memory (RAM) and read-only memory (ROM) as well. The endurance of the device as RAM was examined using write/read/erase/read (W/R/E/R) cycles ( $+4$  V/ $1$  V/ $-4$  V/ $1$  V) in pulse mode (Figure 5). More than 100 cycles with ON/OFF ratios of up to  $10^3$  were observed without any degradation of the device (Figure 6). In addition, after the device was turned ON by applying a positive voltage greater than the threshold value, even with the application of a very small voltage it was tested to maintain the ON state for hours, and a similar kind of behavior was also observed for the OFF state. This indicates the possibility that the device can be used as ROM as well. It is worthwhile to emphasize that the low threshold voltages ( $<3$  V in magnitude) for both the ON and OFF states are desirable for a memory device because they result in low power consumption. They

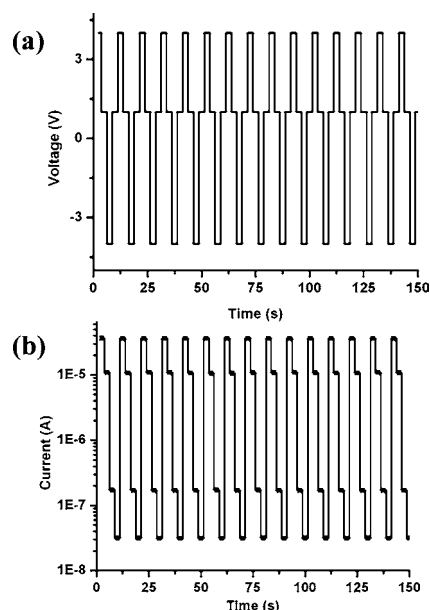


**Figure 5.** (a) Input applied voltage sequence and (b) output current responses during the write/read/erase/read (W/R/E/R) cycle of the gold/[**1b**]CF<sub>3</sub>SO<sub>3</sub>/gold device. Voltages: W,  $+4.0$ ; R,  $1.0$ ; E,  $-4.0$ ; R,  $1.0$  V.

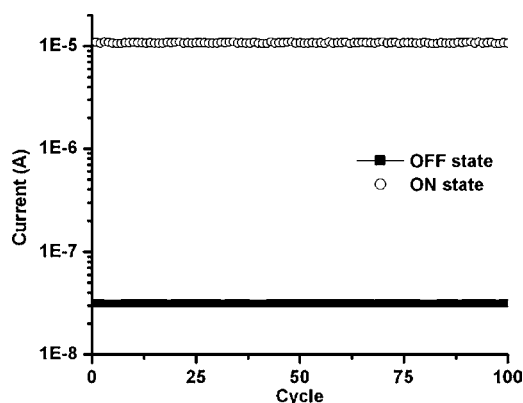


**Figure 6.** Retention times of the ON- and OFF-state data of the gold/[**1b**]CF<sub>3</sub>SO<sub>3</sub>/gold device, probed with currents under  $+1.0$  V. The ON and OFF states were induced by  $+4.0$  (writing) and  $-4.0$  V (erasing), respectively.

may be attributed to the facile multiple redox responses of [**1**]CF<sub>3</sub>SO<sub>3</sub> in the narrow range of applied potential.

In summary, we have reported here a designed synthesis and complete characterization of two unusual but stable triplet azo anion diradical complexes of rhodium(III) differing only with respect to substitution on the coordinated aromatic azo ligand. The diradical complex [**1b**]CF<sub>3</sub>SO<sub>3</sub> showed a pinched hysteresis loop in the  $I$ – $V$  plane, which is a typical feature of a memristive device. On the basis of the simple gold–molecule–gold device structure, we conclude that the switchability and memory phenomena of the azo anion radical memory device originate from the coordinated radical ligands. The device can potentially be used as RAM and ROM, and it exhibits very low area, reduced power consumption, and much higher speed in comparison with devices in practice. While its ON/OFF ratio is not comparable to those of available devices, it is of course reasonably high and comparable to those of several other memristive devices reported<sup>13c,12</sup> in recent times.

Though several useful applications of metal complexes of redox-active radical ligands are currently being investigated,<sup>4a-c</sup> our present results have indeed opened up a heretofore unexplored avenue of research in similar systems.

## ■ ASSOCIATED CONTENT

### ● Supporting Information

Detailed experimental procedures, X-ray crystallographic data (CIF), ORTEP of [1b]CF<sub>3</sub>SO<sub>3</sub>, complete ref 11 (as SI ref 8), and absolute energies and the coordinates of the DFT-optimized structures. This material is available free of charge via the Internet at <http://pubs.acs.org>.

## ■ AUTHOR INFORMATION

### Corresponding Author

icsg@iacs.res.in

### Notes

The authors declare no competing financial interest.

## ■ ACKNOWLEDGMENTS

This research was supported by the Department of Science and Technology (DST), New Delhi (Project SR/S1/IC/0031/2010). Sreebrata Goswami sincerely thanks DST for a J. C. Bose National Fellowship. Crystallography was performed at the DST-funded National Single Crystal Facility at the Department of Inorganic Chemistry, IACS. We are thankful to Dr. S. Malik, Polymer Science Unit, IACS. N.D.P. thanks the Council of Scientific and Industrial Research for fellowship support.

## ■ REFERENCES

- (1) (a) Strukov, D. B.; Snider, G. S.; Stewart, D. R.; Williams, R. S. *Nature* **2008**, *453*, 80. (b) Chua, L. O. *IEEE Trans. Circuit Theory* **1971**, *18*, 507.
- (2) (a) Ouyang, J.; Chu, C.-W.; Szmanda, C. R.; Ma, L.; Yang, Y. *Nat. Mater.* **2004**, *3*, 918. (b) Yang, Y.; Ouyang, J.; Ma, L.; Tseng, R. J.-H.; Chu, C.-W. *Adv. Funct. Mater.* **2006**, *16*, 1001. (c) Scott, J. C.; Bozano, L. D. *Adv. Mater.* **2007**, *19*, 1452. (d) McGinnes, J.; Corry, P.; Proctor, P. *Science* **1974**, *183*, 853.
- (3) (a) Forrest, S. R. *Nature* **2004**, *428*, 911. (b) Waser, R.; Dittmann, R.; Staikov, G.; Szot, K. *Adv. Mater.* **2009**, *21*, 2632. (c) Bandyopadhyay, A.; Sahu, S.; Higuchi, M. *J. Am. Chem. Soc.* **2011**, *133*, 1168.
- (4) (a) Forum on Redox-Active Ligands: *Inorg. Chem.* **2011**, *50*, 9737–9914 and references therein. (b) Tondreau, A. M.; Milsman, C.; Patrick, A. D.; Hoyt, H. M.; Lobkovsky, E.; Wieghardt, K.; Chirik, P. J. *J. Am. Chem. Soc.* **2010**, *132*, 15046. (c) Bart, S. C.; Bowman, A. C.; Lobkovsky, E.; Chirik, P. J. *J. Am. Chem. Soc.* **2007**, *129*, 7212. (d) Buckel, W. *Angew. Chem., Int. Ed.* **2009**, *48*, 6779.
- (5) (a) Chaudhuri, P.; Wieghardt, K. *Prog. Inorg. Chem.* **2001**, *50*, 151. (b) Pierpont, C. G.; Lange, C. W. *Prog. Inorg. Chem.* **1994**, *41*, 331.
- (6) (a) Joy, S.; Krämer, T.; Paul, N. D.; Banerjee, P.; McGrady, J. E.; Goswami, S. *Inorg. Chem.* **2011**, *50*, 9993. (b) Sanyal, A.; Banerjee, P.; Lee, G.-H.; Peng, S.-M.; Hung, C.-H.; Goswami, S. *Inorg. Chem.* **2004**, *43*, 7456. (c) Sanyal, A.; Chatterjee, S.; Castiñeiras, A.; Sarkar, B.; Singh, P.; Fiedler, J.; Zális, S.; Kaim, W.; Goswami, S. *Inorg. Chem.* **2007**, *46*, 8584. (d) Samanta, S.; Singh, P.; Fiedler, J.; Zális, S.; Kaim, W.; Goswami, S. *Inorg. Chem.* **2008**, *47*, 1625. (e) Banerjee, P.; Sproules, S.; Weyhermüller, T.; DeBeer George, S.; Wieghardt, K. *Inorg. Chem.* **2009**, *48*, 5829.
- (7) Paul, N.; Samanta, S.; Goswami, S. *Inorg. Chem.* **2010**, *49*, 2649.
- (8) Saha, A.; Das, C.; Goswami, S.; Peng, S.-M. *Indian J. Chem.* **2001**, *40A*, 198.

- (9) (a) Kahn, O. *Molecular Magnetism*; VCH: New York, 1993. (b) Lu, C. C.; Bill, E.; Weyhermüller, T.; Bothe, E.; Wieghardt, K. *J. Am. Chem. Soc.* **2008**, *130*, 3181. (c) Oshio, H.; Yamamoto, M.; Ito, T.; Kawauchi, H.; Koga, N.; Ikoma, T.; Tero-Kubota, S. *Inorg. Chem.* **2001**, *40*, 5518.
- (10) (a) Brook, D. J. R.; Lynch, V.; Conklin, B.; Fox, M. A. *J. Am. Chem. Soc.* **1997**, *119*, 5155. (b) Gastel, M. V.; Lu, C. C.; Wieghardt, K.; Lubitz, W. *Inorg. Chem.* **2009**, *48*, 2626. (c) Orio, M.; Philouze, C.; Jarjayes, O.; Neese, F.; Thomas, F. *Inorg. Chem.* **2010**, *49*, 646. (d) Devi, S. P.; Singh, R. K. H.; Kadam, R. M. *Inorg. Chem.* **2006**, *45*, 2193.
- (11) Frisch, M. J.; et al. *Gaussian 03*, revision D.01; Gaussian, Inc.: Wallingford, CT, 2004.
- (12) (a) Lee, J.; Lee, E.; Kim, S.; Bang, G. S.; Shultz, D. A.; Schmidt, R. D.; Forbes, M. D. E.; Lee, H. *Angew. Chem., Int. Ed.* **2011**, *50*, 4414. (b) Seo, K.; Konchenko, A. V.; Lee, J.; Bang, G. S.; Lee, H. *J. Am. Chem. Soc.* **2008**, *130*, 2553.
- (13) Hsu, J.-C.; Chen, Y.; Kakuch, T.; Chen, W.-C. *Macromolecules* **2011**, *44*, 5168.